

Pulverised coal/biomass co-fire modelling in a full scale corner-fired boiler

S.R. Gubba¹, D.B. Ingham¹, K.J. Larsen¹, L. Ma^{1,*}, M. Pourkashanian¹, H.Z. Tan^{1,2}, and A. Williams¹

¹Centre for Computational Fluid Dynamics, School of Process, Environmental and Materials Engineering, University of Leeds, Leeds, LS2 9JT, UK

²State Key Laboratory of Multiphase Flow in Power Engineering, School of Energy and Power Engineering, Xi'an Jiaotong University, Xi'an 710049, China

Abstract

The practice of co-firing biomass in full-scale coal utility plants is gradually increasing. This is mainly because of the benefits associated in reducing the coal based CO₂ and biomass based SO_x and NO_x emissions. Significant numbers of existing coal power stations are suitable for co-firing with small/no changes in the original infrastructures. In order to demonstrate this, combustion modelling of a 300MWe, widely used tangentially fired furnace for pulverised coal has been undertaken in this work. Typical Chinese fuels, Huating coal and wheat straw, were burned at 100% coal and under coal/wheat straw co-firing (up to ≈12.5% on a thermal basis). In the experiments, wheat straw has been handled by the existing coal mills and feeding system to a set of dedicated burners. CFD predications are in good agreement in general with the measured data such as temperature, furnace exit oxygen, unburnt carbon in the ash and NO_x emissions.

Keywords: Biomass; co-firing; pulverised fuel; large scale; CFD modelling

Introduction

Coal continues to provide a major source for electricity generation. The total world coal consumption was approximately 138EJ (4.9Gt of anthracite) [1] and represents 29.4% of world primary energy consumption, its greatest proportion since 1970 [1]. This figure rises to

* Corresponding author: Tel.: +44 113 3432481; Fax: +44 113 2467310

Table 1. Test conditions of biomass co-firing

Case	Case 0	Case 1	Case 2
Total output power (MWth)	629	652	660
Coal mass flow rate (kgs ⁻¹)	31.94	31.11	29.44
Straw mass flow rate (kgs ⁻¹)	0.00	3.33	6.67
Co-fire thermal load	0.00%	6.21%	12.35%
Excess oxygen (dry vol.)	3.0%	4.1%	3.7%
NO _x emissions (ppm)	242	222	214

almost 40% of world electricity generation, which has grown at a faster rate than primary energy over the past 40 years [2]. Co-firing coal with biomass at existing power stations offers an opportunity for an increase in renewable energy generation because of concerns arising from CO₂ emissions. Pulverised fuel power stations demonstrate a flexible method for co-firing retrofit [3].

China is the largest agricultural country in the world with over 35Mt of cotton, corn and wheat straw residues, highly suitable for pellets or briquettes, being produced in China in 2006 [4]. Numerous studies have investigated the computational modelling of full scale coal power stations, many of a similar design to that of the present study [5-8], however there are far fewer studies on such a scale for co-firing. A detailed study of air staging for tangential firing in a 1MWe boiler is presented by Li et al. 2009 [9] and a small scale test furnace employing a single low NO_x swirl burner was investigated under co-firing conditions by Damstedt et al. 2007 [10]. Battista et al. 2000 [3] present experimental measurements from a US 150MWe tangentially fired pulverised coal power unit, originally built in the 1950s, which is co-fired with up to 14% sawdust, on a thermal basis, using separate injection. Wang et al. 2011 [11], the basis of the current investigation, also considered the effect of biomass on the coal feeding system by selecting separate injections to a set of dedicated upstream burners. All the above studies [10-12] conclude that the co-firing with biomass would not reduce the fuel feed capacity and offers significant NO_x reductions with promising economy. Furthermore the economic capability would increase for larger and more efficient units providing the biomass can be supplied and the heat transfer in the boiler is not reduced.

In the present study, Computational Fluid Dynamics (CFD) is used to model the full scale 300MWe tangentially fired furnace [11] for pulverised fuel (coal and wheat straw). One main reason to choose corner fired furnace in this study is because it is widely employed by existing coal power stations. The main objective of this investigation is to simulate various test conditions as presented in [11] and to understand various physical and chemical processes by analysing the CFD data. Also, this study facilitates as a platform, so future studies will aim to develop more models for a better understanding.

Experimental Test Case

The experiments were performed on a 300MWe furnace at the Baoji power station, Shaanxi, China. The details are presented in [11], however an overview is provided in this paper. The

furnace employs three distinct banks of burners, each composed of three secondary air inlets interposed by two primary air inlets. The highest of these banks also incorporates a close-coupled over-fire air (OFA) inlet above. The OFA is injected into the boiler to give an opposite rotational direction of the fireball, in the recirculation zone, compared to the other inlets. The three banks are present in the four corners, which come 64 inlets, although these are not all operated simultaneously under the firing conditions in this study. The system provides the means for air staging and a recirculation zone above the burners. The cases studied are summarised in Table 1. A baseline test of typical operation of the furnace, firing coal only (Case 0), was first performed. Thereafter a battery of coal mills, used to supply the top primary air conveyers, was given over to biomass processing at 12 or 24 t/h (3.33 or 6.67 kgs^{-1} ; Cases 1 and 2, respectively). For comparison, the system used for the wheat straw is capable of handling approximately 9 kgs^{-1} of coal. In the separate injection method of co-firing the co-fired fuels are mixed only upon entrance to the boiler. It is important to note that the power station was designed to burn only coal and that no modifications have been made to the hardware, except the biomass storage and onsite handling. This represents a simple and cheap retrofit co-firing configuration for many similar furnace designs that have burners with dedicated upstream fuel systems.

Huating bituminous coal, the design fuel for the furnace, was employed in all cases. Measured fuel properties, as used in the numerical calculations, are presented in Table 2. The biomass used was local pelletised wheat straw. Pellets alleviate the difficulties that usually arise in handling and milling of low energy density fibrous biomass, on site, as well as transportation of the fuel. However, the pellets must be milled to derive straw particles of a suitable size. Even moderate co-fire loadings employed herein require a significant biomass resource necessitating a wide catchment area and an extensive network of transportation. In the pelletising process, the requirement that a binding agent be used resulted in soil, a quarter of the mass of straw, being added. This explains the undesirable ash content in Table 2. Straw is widely used as a fuel in China. A slight decrease in the temperatures and carbon burnout is reported under co-firing, the cases examined here are closely comparable, the input-heat varies by less than 5% amongst them but greater excess air is present under the biomass combustion conditions.

Numerical Input

The chemical properties and composition of the fuels are predicted from their proximate and ultimate analyses, as given in Table 2. The sulphur content is small and therefore omitted from the calculations. The fuel samples must be taken as representative, although meteorological effects and processing can induce profound variability, particularly in biomass. Logarithmic Rosin-Rammler size distributions are fitted to sieved coal particle size classes and optically measured straw particle sizes as given in Table 3 for the coal, and the straw samples provided at the two milling rates.

The mass flow rate of the fuels and the lower velocities in the primary air were measured.

Table 2. Proximate and ultimate analysis of the tested fuel.

	Proximate Analysis % AR				Ultimate Analysis % DAF				HCV (MJkg ⁻¹)
	FC	VM	A	M	H	O	N	C	
Huating Coal	41.6	25.1	17.3	16.0	4.6	15.1	0.8	79.5	20.65
Straw	12.2	46.9	28.3	12.6	3.0	34.1	2.6	60.3	13.15

Table 3. Coal and biomass particle properties

Rosin-Rammler	Huating Coal	Straw (12t/h)	Straw (24t/h)
Parameters	Cases 0, 1 & 2	Case 1	Case 2
Min. diameter (μm)	50	50	50
Max. diameter (μm)	300	1500	1500
Mean diameter (μm)	70	100	450
Spread parameter	1.2	1.2	1.3
Dry density (kgm ⁻³)	1300	500	500

The total mass flow rate of the air used in the calculations is determined based on the desired excess air and the stoichiometry of the fuel and air, based on the ultimate analysis. This is distributed between the inlets in proportion to their respective velocity measurements. At each inlet this air is injected at an angle that is tangential to the fireball with known radii and in an anti-clockwise direction – except at the OFA which takes the opposite, clockwise, direction. The particles enter with the same velocity as the air. To simulate the physical conditions, the air is preheated to 350 and 570K for primary air and secondary air, including OFA, respectively in the numerical calculations.

Data was not available for the furnace wall temperatures. It was therefore formulated as a profile ranging between the saturation and maximum temperature expected in the steam plus a 50K temperature difference, assumed by the experimental operator, for the steel (690 – 750K). The maximum temperatures of the wall profile and the estimated temperature distribution along the height of the boiler coincide. Assuming the steam flow rate reduces from the design value in proportion to the coal consumption for the baseline, case 0, the total latent heat that must be supplied to raise the steam in the furnace walls at saturation temperature is 180MW. Note that this does not include heat through the super heater which is placed downstream of the burner region in which the dominant physical processes occur. The same temperature profile in the wall is used for all three cases. The wall emissivity has been taken to be 0.5.

Numerical Models

The CFD modelling is performed using ANSYS FLUENT 12.1 [13] with eight parallel processors, 4GB RAM on a centralised Linux cluster. The simulated domain is large with a cross section of approximately 14 x 15 m in the recirculation region with a height of 55 m,

thus having a volume of about 11200m³. The mesh uses four million grid points with relatively higher grid densities in the near burner regions, where most of the combustion and heat transfer is expected to occur.

Steady RANS calculations are performed using the realisable κ - ϵ model [13] with scalable wall functions. The volume of the cells adjacent to the wall is similar to their neighbouring cells, this is unavoidable but tolerable as the wall-turbulence and convective heat transfer effects are of less importance than combustion-turbulence and radiative heat transfer in hot combusting flows. The radiation is modelled by the discrete ordinate method. Coal and biomass particles are tracked by Lagrangian approach in the 3D domain, assuming all the particles are of spherical shape. For particle combustion moisture evaporation, devolatilisation and char combustion are sequentially modelled. During these the mass of moisture, volatiles and the majority of fixed carbon is lost from the particle with the ash and unburnt carbon remaining.

An overall devolatilisation step is used to determine the devolatilisation of the coal and biomass particles; the volatile matter consists of the yield of gas and tar. A first-order single step Arrhenius equation is used to predict the rate of devolatilisation. The rate constants for a typical bituminous coal and measured pulverised wood published in [14] are used in the present investigation. The wood and straw particles from the different studies were identified to have a similar size distribution. The rates of coal and wood devolatilisation are similar to bituminous coal and wheat straw values [15], although at high heating rates in real furnaces, $\approx 10^5 \text{Ks}^{-1}$, the constants used to describe the rate of devolatilisation are less critical [16]. Char combustion assumes a pure carbon one-step oxidation reaction. In the case of coal this is limited by both the gaseous oxygen diffusion and the intrinsic reactivity of the coal char based on Smith's method and using suggested reaction properties supplied by a comprehensive study of a range of bituminous coals [17, 18]. Biomass char combustion is modelled as limited by the diffusion of locally depleted O₂ to the surface of the straw char particles, which will be much larger [19]. Also the intrinsic reactivity of biomass will remain greater than that of coal [17- 20]. Biomass char may alternatively be modelled using Smith's model but increasing the reaction twofold [14]. An eddy dissipation model is used for volatile combustion and is used to couple turbulence and chemical reactions in order to calculate the gas reaction rates.

NO_x formation is predicted by post-processing using the models described in our earlier publication [17]. The key sources of NO_x for solid fuel combustion at high temperatures are, in order, fuel-N and thermal-N. It has been found that biomass chars retain a greater proportion of the original fuel-N than those of coal [20] although Glarborg et al. 2003 [21] suggest that this trend is reversed at furnace temperatures.

Results and Discussion

Table 4. Comparison of experimental data and numerical predictions.

Results		Case 0		Case 1		Case 2	
		Exp	Num	Exp	Num	Exp	Num
Temperature (K) at various furnace heights* (m)	34.0	1621±25	1490	1593±25	1515	1598±25	1530
	37.0	1573±25	1445	1551±25	1470	1559±25	1485
	48.3	1388±25	1310	1378±25	1325	1381±25	1340
Excess oxygen (dry, volumetric)		3.0%	2.6%	4.1%	3.6%	3.7%	3.2%
Unburnt carbon in ash (mass)		0.18%	0.04%	0.47%	0.00%	0.52%	0.00%
NO _x (dry, ppm)		242	232	222	189	214	185

*The listed heights include a 6.9m displacement of the bottom of the numerical domain above the ground, therefore height 48.3m is actually \approx 13m from the furnace ceiling).

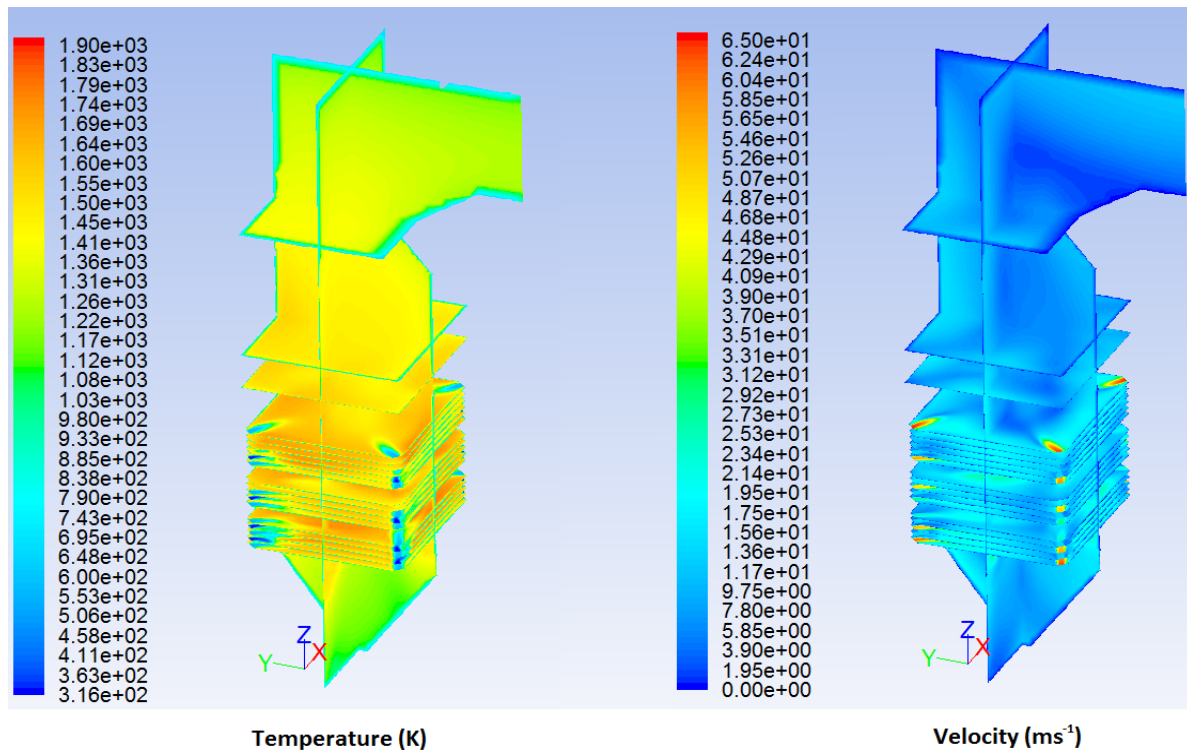


Figure 1. Typical images of the temperature and velocity contours for case 0 (100% Coal). Contour legend is shown on the left hand side of each image.

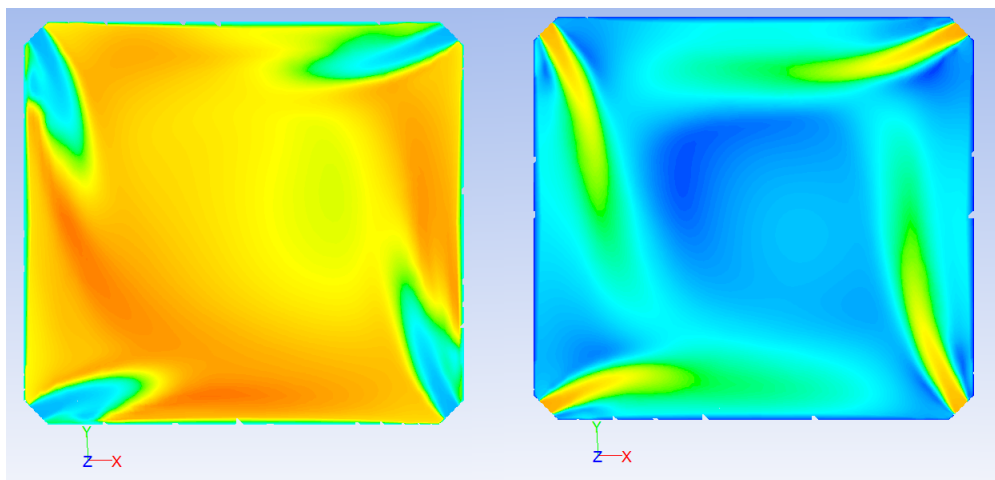


Figure 2. Typical inlet planes of the corner fired furnace, demonstrating the anti-clockwise rotation of the fireball. The image on the left shows the temperature contours and the right shows the velocity contours. The legend for temperature and velocity is as shown in Figure 1.

In this section the CFD predictions obtained from this investigation are presented and compared with the published experimental data [11]. Table 4 presents a comparison of the experimental data and numerical predictions of the gas temperatures, excess oxygen content at exit, unburnt carbon in ash and NO_x . Figure 1 presents predicted contours of the temperature and velocity in the corner fired furnace at important vertical and horizontal

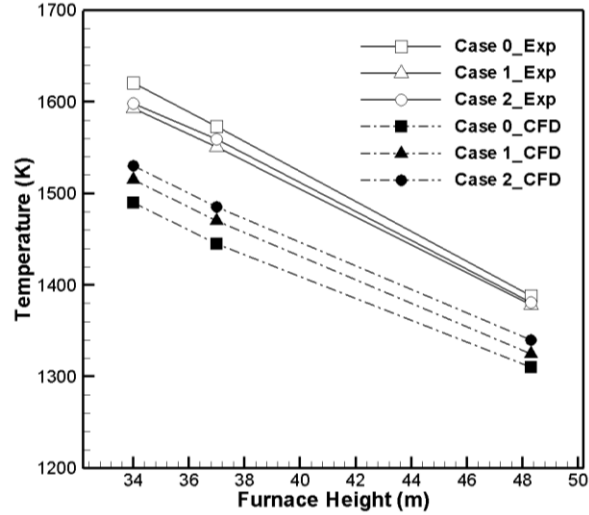


Figure 3. Comparison of the temperature predictions with the measured data against furnace height for Cases 0, 1 and 2.

planes for Case 0. The horizontal planes in Figure 1 highlight the locations of the sixteen velocity inlets (lower) and the three measurement locations (upper) as in Table 4. Figure 2 presents the predicted temperature and velocity contours of a typical inlet plane, demonstrating the anti-clockwise rotation of the fireball. Similar images from other two cases utilising biomass may be presented here. However, it was noticed that the differences in the contour plots between Cases 0, 1 and 2 are of less significance due to the computational volume of the domain considered in this investigation.

Figure 3 presents temperature predictions for Cases 0, 1 and 2 against the measured data at three different furnace heights (34, 37 and 48.3 m). It is clear that the CFD predictions of the temperatures profiles are in reasonable agreement with the measured data and follow the same trend, *i.e.* decreasing along the furnace height. Although the CFD predictions of gas temperatures were consistently under-predicted, the maximum discrepancy between the predictions is observed to be about 8% of the measured value. This is thought to be mainly due to the thermal boundary condition at the wall used in this investigation and this may have been too severe. Further, the temperatures are measured by infrared sensors and whereas the temperature predictions are of mass-weighted average across the plane at the respective measurement heights. Figure 3 also confirms the effect of the biomass feeding rates on the temperature profiles along the height of the furnace. The trend of the predicted temperatures follows the total-heat input so the trend in Cases 1 and 2 with 12 and 24 t/h feeding rates of biomass is consistent with measurements and the temperature at various heights is found to be higher with higher feeding rate of biomass.

The predicted excess oxygen (dry volumetric O_2 fraction at the exit) presented in Table 4 is also in reasonable agreement compared to the measured data. It should be noted that there are difficulties associated in obtaining the experimental measurements at the precise location at which the sample is taken. Moreover, the amount of air leak-in into the furnace is not clearly known and therefore this has not been considered in the present modelling. However, experience suggests that the air leak-in in industrial furnaces will be at least about 5 to 20 % of the total air intake, which is not an insignificant amount.

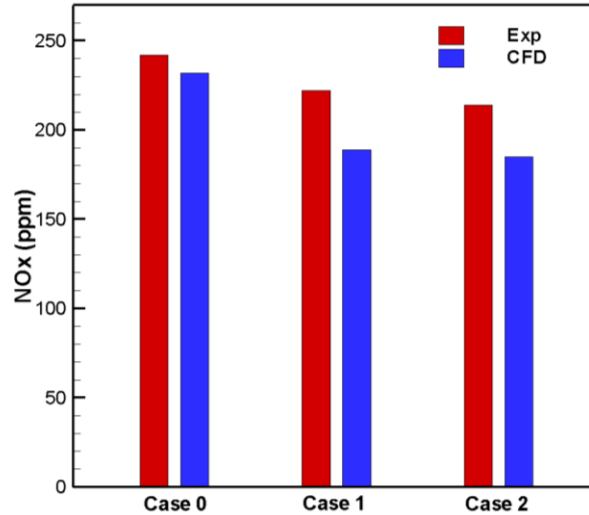


Figure 4. Comparison of the dry NO_x predictions with the measured data for Cases 0, 1 and 2.

The amount of unburnt carbon in the ash is another important parameter presented in Table 4 from both the measurements and predictions. It is clear that unburnt carbon in the ash has been under-predicted in all the cases compared to measured amounts. One reason for this is the particles shape and their distribution considered in this investigation. All wheat straw particles were considered as equivalent spherical particles, which simplifies the drag experienced by the particle and the heat transfer, and thereby causing devolatilisation and char combustion of particles well within the particle residence times. Moreover, a standard method was used to select the Rosin-Rammler particle size distribution parameters, but resulted in a small number of classes and very large volume fraction in a single class caused smaller particle sizes to be unfairly weighted.

Measured NO_x emissions have been reported in our previous investigation [11]. NO_x emissions are a major concern for power station operation, and may play a role in the economics of co-fire retrofitting [3]. Therefore accurate predictions are vital to prove a numerical benchmark. Figure 4 presents a comparison of the predicted and measured NO_x in ppm dry for Cases 0, 1 and 2. It is clear that the CFD predictions are capable of reproducing the NO_x trend in line with the experiments showing the effect of biomass co-firing in the furnace. With the increase of biomass feed rate in Case 2 to 24t/h, the NO_x emissions have been predicted to reduce by about 20% compared to 11% reduction in experiments. Although the NO_x predictions were slightly under-predicted, CFD calculations demonstrate the reduction in NO_x as expected in co-firing conditions compared to 100% coal conditions. One main reason for the under-predictions is thought to be high dependency of NO_x on the furnace temperatures and oxygen concentration in modelling, which is slightly under-predicted in this investigation. Further, the decrease in the volatile fuel-N, on a thermal basis is expected to influence NO_x predictions. However, the errors in the predictions are tolerable with the current assumptions in the modelling.

Summary

Co-firing of the coal and wheat straw in a 300MWe tangentially fired furnace has been modelled using CFD techniques. Experimentally measured data in the same furnace under baseline and differing co-fire loadings have been used to assess the sophistications required for computational modelling of such a large and elaborate system. Despite the simplifications assumed in the CFD modelling, the predictions were, in general, in reasonable agreement with measurements. In particular, the predicted temperature profiles and excess oxygen at the exit are very promising, considering the uncertainty that exists for the thermal boundary conditions both in terms of wall temperature, emissivity, and no air leak-in in large scale industrial boilers. Increase in the gas temperature along the furnace height with the increase in biomass feed rate from 12 to 24 t/h is clearly demonstrated by CFD and is in good agreement with experiments.

It is postulated that the discrepancies in predicted carbon burnout compared to the measured data in Cases 0, 1 and 2 is mainly due to the particle shapes and unrepresentative particle size distributions considered. Further, the devolatilisation and char combustion parameters used for wheat straw are expected to greatly influence the predictions. NO_x predictions for all the cases considered in this investigation are in good agreement with the measurements demonstrating the reduction in NO_x with co-firing of biomass.

Overall, encouraging results have been obtained from the CFD calculations in all the cases, including co-firing at various feed rates. The necessity of detailed inputs of the biomass particles shape, distribution and their thermal conversion behaviours is clearly identified to influence the CFD predictions and further work is required to address these issues. This study also addresses the importance of model development for the prediction of ash deposition, slagging and fouling in industrial furnaces using pulverised biomass co-firing, and this will make a valuable next step.

Acknowledgements

The CFD investigations were carried out at Leeds University, Leeds, UK with the financial support from the EPSRC grant (EP/F061188/1). Experimental investigations were carried out in China with the financial supported from the Natural Science Foundation of China (No. 50976086). Also the authors acknowledge the Baoji power station, Shaanxi, China for providing experimental test facilities.

References

1. BP Statistical Review 2010. www.bp.com [February 2011]
2. OECD Factbook 2010. www.oecd-ilibrary.org [February 2011]
3. Battista JJ, Hughes EE, Tillman DA. Biomass co-firing at Seward station. *Biomass and Bioenergy* 2000; 19:419-427

4. Cai JM, Liu RH, Deng CJ, Shen F. Amount, availability and potential uses for energy of agricultural residues in mainland China. *Journal of the Energy Institute* 2007; 80(4):243-246
5. Backreedy RI, Jones JM, Ma L, Pourkashanian M, Williams A, Arenillas A, Arias B, Pis JJ, Rubiera F. Prediction of unburned carbon and NO_x in a tangentially fired power station using single coals and blends. *Fuel* 2005; 84:2196-2203
6. Belosevic S, Sijercic M, Tuckovic D, Crnomarkovic N. A numerical study of a utility boiler tangentially-fired furnace under different operating conditions. *Fuel* 2008; 87:3331-3338
7. Díez LI, Cortés C, Pallarés J. Numerical investigation of NO_x emissions from a tangentially-fired utility boiler under conventional and overfire air operation. *Fuel* 2008; 87:3331-3338
8. Choi CR, Kim CN. Numerical investigation on the flow, combustion and NO_x emission characteristics in a 500MWe tangentially fired pulverised-coal boiler. *Fuel* 2009; 88:1720-1731
9. Li S, Xu T, Hui S, Zhou Q, Tan H. Optimisation of air staging in a 1MW tangentially fired pulverised coal furnace. *Fuel Processing Technology* 2009; 90:99-106
10. Damstedt B, Pederson JM, Hansen D, Knighton T, Jones J, Christensen C, Baxter L, Tree D. Biomass co-firing impacts on flame structure and emissions. *Proceedings of the Combustion Institute* 2007; 31:2813-2820
11. Wang X, Tan H, Niu Y, Pourkashanian M, Ma L, Chen E, Liu Y, Liu Z, Xu T. Experimental investigation on biomass co-firing in a 300MW pulverised coal-fired utility furnace in China. *Proceedings of the Combustion Institute* 2011; 33:2725-2733
12. Sami M, Annamalai K, Wooldridge M. Co-firing coal and biomass fuel blends. *Progress in Energy and Combustion Science* 2001; 27:171-214
13. ANSYS FLUENT, Version 12, Ansys Inc. USA, 2009.
14. Ma L, Jones JM, Pourkashanian M, Williams A. Modelling the combustion of pulverised biomass in an industrial combustion test furnace. *Fuel* 2007; 86:1959-1965
15. Williams A, Pourkashanian M, Jones JM. Combustion of coal and biomass. *Progress in Energy and Combustion Science* 2001; 27:587-610
16. Saddawi A, Jones JM, Williams A, Wójtowicz MA. Kinetics of thermal decomposition of biomass. *Energy and Fuels* 2010; 24:1274-1282
17. Backreedy RI, Fletcher LM, Ma L, Pourkashanian M, Williams A. Modelling pulverised coal combustion using a details coal combustion model. *Combustion Science and Technology* 2006; 178:763-787
18. Darvell L, Jones JM, Saddawi A, Williams A. To be published.
19. Gera D, Mathur M, Freeman M, O'Dowd W. Moisture and char reactivity modelling in pulverised coal combustors. *Combustion Science and Technology* 2001; 172:35-69
20. Wornat MJ, Hurt RH, Yang NYC, Headley TJ. Structural and compositional transformations of biomass chars during combustion. *Combustion and Flame* 1995; 100:131-143
21. Glarborg P, Jensen AD, Johnsson JE. Nitrogen conversion in solid fuel fired systems. *Progress in Energy and Combustion Science* 2003; 29:89-113